Materials
Views
www.MaterialsViews.com

ADVANCED
ENERGY
MATERIALS
www.advenergymat.de

FULL PAPER

Interdiffusion of PCBM and P3HT Reveals Miscibility in a Photovoltaically Active Blend

Neil D. Treat, Michael A. Brady, Gordon Smith, Michael F. Toney, Edward J. Kramer, Craig J. Hawker,* and Michael L. Chabinyc*

Developing a better understanding of the evolution of morphology in plastic solar cells is the key to designing new materials and structures that achieve photoconversion efficiencies greater than 10%. In the most extensively characterized system, the poly(3-hexyl thiophene) (P3HT):[6,6]-phenyl-C_{61}-butyric-acid-methyl-ester (PCBM) bulk heterojunction, the origins and evolution of the blend morphology during processes such as thermal annealing are not well understood. In this work, we use a model system, a bilayer of P3HT and PCBM, to develop a more complete understanding of the miscibility and diffusion of PCBM within P3HT during thermal annealing. We find that PCBM aggregates and/or molecular species are miscible and mobile in disordered P3HT, without disrupting the ordered lamellar stacking of P3HT chains. The fast diffusion of PCBM into the amorphous regions of P3HT suggests the favorability of mixing in this system, opposing the belief that phase-pure domains form in BHJs due to immiscibility of these two components.

1. Introduction

Bulk heterojunction (BHJ) organic photovoltaics (OPV) have recently achieved photoconversion efficiencies approaching 10% through the synthesis of electron-donating polymers and the empirical optimization of the processing conditions of the active layer.[1] Further improvement in efficiency is limited by a lack of a fundamental understanding of the morphology (i.e. size, shape, texture, and phase distribution) of the donor and acceptor phases within a BHJ film. Thus, there is a need to develop a fundamental understanding of the miscibility and diffusivity of the donor and acceptor components within these films with the ultimate goal of a detailed understanding and the ability to control molecular ordering and phase separation. Here, by using a model bilayer system of P3HT and PCBM, we observe rapid (30 s) interdiffusion of pure layers of P3HT and PCBM at typical OPV annealing temperatures (150 °C). Significantly this mixing occurs without disrupting the crystalline P3HT domains and is indicative of the miscibility of PCBM in disordered P3HT domains. Our results imply that the BHJ film is comprised of a dispersion of aggregates of PCBM, molecularly dispersed PCBM in disordered P3HT, and crystallites of P3HT and suggests that the pure polymer domains widely thought to exist in BHJ films are, in fact, disordered solutions of crystalline and disordered polymer and amorphous fullerene.[2]

The most efficient OPVs are formed from blends of an electron-donating polymer [e.g. poly(3-hexyl thiophene) (P3HT)] and an electron-accepting fullerene {e.g. [6,6]-phenyl-C_{61}-butyric-acid-methyl-ester (PCBM)}.[3] The efficiency of BHJs relies on the ability of photogenerated excitons to reach the heterojunction between the donor and acceptor, generating free charge carriers, coupled with the ability of these charge carriers to escape to the electrodes. The first factor requires the donor and acceptor to be dispersed within a maximum distance of ~10 nm due to the limited diffusion distance of the excitons and the latter requires efficient pathways of hole and electron transport to the electrodes over distances of 100–500 nm.[4] Currently, the phase-separated morphology is difficult to control and empirical processing methods are relied upon to form highly efficient OPVs.

Although the P3HT:PCBM BHJ is the most extensively studied BHJ[4–7,11], its internal structure is still a topic of intense debate. P3HT:PCBM BHJs[8] are commonly deposited from solution *via* spin-coating onto a high work function transparent conducting oxide (i.e. ITO) coated with a water soluble, hole conducting layer (i.e. PEDOT:PSS).[4] The as-cast blend morphology is generally believed to be a kinetically trapped molecular mixture of P3HT (both amorphous regions and crystalline

N. D. Treat, M. A. Brady, Prof. E. J. Kramer, Prof. C. J. Hawker, Prof. M. L. Chabinyc
Materials Research Laboratory
University of California Santa Barbara
Santa Barbara, CA 93106, USA
E-mail: hawker@mrl.ucsb.edu; mchabinyc@engineering.ucsb.edu
N. D. Treat, M. A. Brady, G. Smith, Prof. E. J. Kramer,
Prof. C. J. Hawker, Prof. M. L. Chabinyc
Materials Department
University of California Santa Barbara
Santa Barbara, CA 93106, USA
Prof. E. J. Kramer
Department of Chemical Engineering
University of California Santa Barbara
Santa Barbara, CA 93106, USA
G. Smith
Department of Chemistry & Biochemistry
University of California Santa Barbara
Santa Barbara, CA 93106, USA
Dr. M. F. Toney
Stanford Synchrotron Radiation Lightsource
2575 Sand Hill Road, MS: 99, Menlo Park, California, 94025, USA

www.MaterialsViews.com

ADVANCED
ENERGY
MATERIALS
www.advenergymat.de

FULL PAPER

regions) and aggregates of PCBM.[9] These films typically have low photoconversion efficiencies, which are attributed to inefficient charge transport pathways due to incomplete phase segregation.[10] In order to achieve optimum charge transport, this system is subjected to processes such as thermal annealing that allow for the reorganization of the bulk heterojunction.[5,9] Some suggest that this increase in performance is due to crystallization of disordered P3HT, resulting in the diffusion of the fullerene component out of the polymer matrix thereby forming efficient charge transport pathways between the electrodes.[12] Others speculate that the increase in the polymer crystal size during thermal annealing inhibits the evolution of large fullerene domains, thus forming nano-scale crystalline domains of P3HT and PCBM.[13] Even though insight into this system has grown tremendously, the understanding of the evolution of the BHJ morphology and improvement in photoconversion efficiency with thermal annealing remains poorly understood.

The aim of this work is to develop a fundamental understanding of the miscibility of P3HT and PCBM by investigating the interdiffusion and mixing processes starting from a bilayer film. From the evolution of the morphology in this model system, a better understanding of the distribution of the active layer components within the bulk heterojunction can be obtained. We find that interdiffusion within P3HT/PCBM bilayers occurs at relatively low temperatures (i.e. 50 °C) and rapidly (30s) results in a mixed system (greater than a 1:0.8 wt ratio) at temperatures commonly used to optimize photovoltaic cells (150 °C). This rapid interdiffusion rate gives evidence that PCBM mixes as molecular species or small aggregates, thus supporting the idea that the BHJ morphology is very dynamic with significant molecular mobility under widely-used annealing conditions.[14] Furthermore, PCBM diffuses within the film without affecting the crystal size, structure, or orientation of P3HT, even at an equal P3HT:PCBM weight ratio. This result suggests that diffusion occurs only through the disordered regions of P3HT. The fast interdiffusion rate observed in the P3HT:PCBM bilayer sheds light on the challenges in controlling the vertical composition of solar cells with either a bilayer geometry or a conventional geometry with blocking layers. Our studies also demonstrate that the bulk has a nearly homogeneous vertical profile (not including differences in concentration at the substrate or air interface as described below), even when starting from the most stratified case. These studies outline the criteria required to fabricate a bilayer system with pure donor and acceptor layers, which is important for the development of model systems for fundamental studies of photophysical and electrical properties.

2. Results and Discussion

2.1. Fabrication and Characterization of P3HT/PCBM Bilayers

For this study, bilayers of P3HT/d-PCBM were fabricated using a float-casting technique to study the evolution of the interface between the P3HT and PCBM upon thermal annealing (details in Experimental section). Films of P3HT and PCBM were separately fabricated *via* spin coating and had approximate thicknesses of 265 nm and 180 nm respectively, yielding at least a 1:0.8 weight ratio assuming the densities of P3HT and PCBM are 1.15 g/mL and 1.3 g/mL respectively.[15] The lowest reported value for the density of PCBM (ranging from 1.3 g/mL to 1.5 g/mL[16]) was used in the estimation of the weight ratio to avoid overestimating the miscibility within this system. Neat P3HT and PCBM films were allowed to age for 2 days at room temperature in an inert environment before bilayer fabrication so that each film had an identical aging history. The P3HT film was then floated onto a deionized (DI) water surface and picked up by the supported PCBM film, forming a bilayer of P3HT/PCBM on an SiO_2/Si substrate. The composition of the P3HT/PCBM bilayer samples was characterized using a combination of dynamic secondary ion mass spectrometry (DSIMS) and cross-sectional scanning electron microscopy (SEM) (**Figure 1**). It was convenient to use ^2H labeled PCBM due to the excellent sensitivity for detecting ^2H by DSIMS. The ^2H profile (Figure 1b)
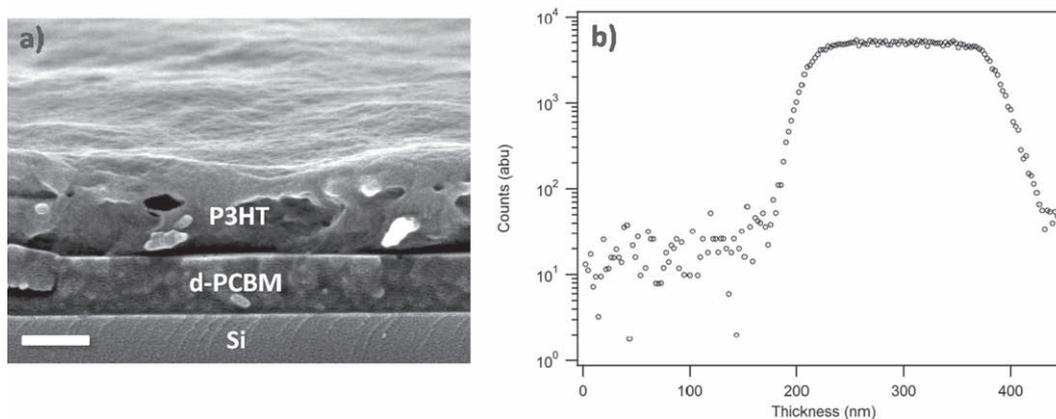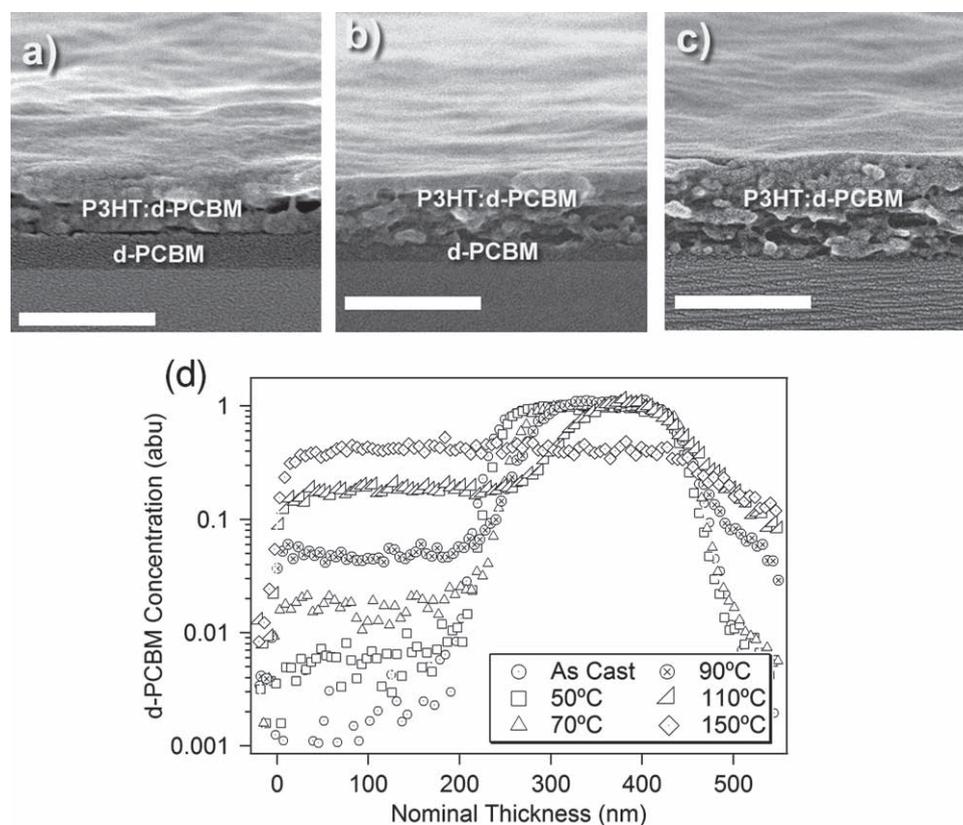

Figure 1. a) Cross-sectional SEM image and b) DSIMS profile of ^2H in a P3HT/d-PCBM bilayer film fabricated on an SiO_2/Si substrate. The sharp change in the ^2H signal from natural abundance signifies the presence of pure P3HT and d-PCBM layers, confirmed by the difference in texture observed in the cross-section SEM image. Profiles were generated using O_2^+ primary ion beam and had a depth resolution of ~10 nm. The thicknesses of the films were determined using an average etch rate of 0.4 nm/s (determined by film thickness studies) and set such that 0.0 is the free surface of the film and 400 nm is the substrate. The scale bar represents a distance of 200 nm.

is plotted as counts versus thickness, clearly showing that there are two distinct layers within the sample. Furthermore, the ^{2}H concentration within the P3HT film corresponds to the natural abundance of deuterium (0.015% of ^{1}H) signifying a pure layer of P3HT (See Supporting Information). The width of the interface between P3HT and PCBM layers is ~10 nm, which is approximately the depth resolution of DSIMS. Concurrently, the cross-section SEM image shows a clear interface and distinguishable difference in texture between the P3HT and d-PCBM films. Other methods for the fabrication of bilayer samples (i.e. direct casting from orthogonal solvents) were unable to form a pure bilayer structure (See Supporting Information).[17] It should be noted that others have shown the fabrication of bilayer type devices with pure donor-acceptor layers using alternate methods.[18] Thus, to fabricate a pure bilayer system, it is important to use solvent free techniques which require no additional heating during the fabrication process (as discussed below).

2.2. Interdiffusion Within P3HT/PCBM Bilayers

The interdiffusion of PCBM and P3HT in this bilayer architecture (P3HT/d-PCBM on SiO$_2$ (150 nm)/Si) at different

annealing temperatures at fixed time was investigated using cross-sectional SEM and DSIMS.[19] **Figure 2d** shows the DSIMS profiles plotted as d-PCBM concentration versus nominal thickness. The increase in d-PCBM concentration within the P3HT layer, as revealed by depth profiles, demonstrates significant interdiffusion at all annealing temperatures (e.g. 10 wt% PCBM in P3HT at 90 °C after 5 min) with complete interdiffusion after 5 min at 150 °C. Similar profiles were observed even when heating at 150 °C for 30 sec, suggesting rapid interdiffusion (Supporting Information). Although the bulk had a uniform composition, a concentrated P3HT layer and a PCBM layer (~10 nm thick) were observed at the air and substrate interfaces respectively, similar to previous reports (Supporting Information).[15,20] Rapid interdiffusion was confirmed by cross-sectional SEM images, revealing that the original interface moves towards the substrate with increasing annealing temperature and is no longer visible after annealing at 150 °C for 5 min (Figure 2a–c). At lower annealing temperatures, a sharp increase in PCBM concentration at the interface between the P3HT and PCBM layers reveals that an interface still exists between an intermixed P3HT-rich layer and nearly pure d-PCBM layer. As interdiffusion proceeds, the interface moves towards the Si substrate, signifying the increase in volume of the P3HT layer due to the inclusion of d-PCBM.

Figure 2. Cross sectional SEM images of a P3HT/d-PCBM bilayer on a silicon wafer annealed at a) 70 °C, b) 110 °C, and c) 150 °C for 5 min. The scale bar represents a distance of 200 nm. d) DSIMS profiles of ^{2}H in bilayer samples of P3HT and d-PCBM annealed from 5 minutes at different temperatures. The thicknesses of the films (which differed slightly across samples) were normalized such that 0 nm is the free surface of the film and 450 nm is the substrate. The deuterium concentrations were normalized such that the area under the counts versus distance for all profiles was the same after setting the normalized concentration in the d-PCBM part of the initial bilayer equal to 1.

www.MaterialsViews.com

ADVANCED
ENERGY
MATERIALS
www.advenergymat.de

FULL PAPER

The fact that there is no d-PCBM concentration gradient in the P3HT-rich layer at all temperatures signifies that there is very rapid diffusion of d-PCBM in the P3HT layer.[21] Since the interdiffusion process is complete at 150 °C for 30 sec, it is clear that the interdiffusion coefficient for this system must be greater than 3×10^{-10} cm^2/s (See Supporting Information) at 150 °C. Diffusion constants for PCBM within a P3HT matrix have also been measured by studying the depletion of PCBM from the P3HT matrix surrounding a PCBM crystalline domain and shown to be 2.5×10^{-10} cm^2/s, which is consistent with our estimate for the lower limit of the interdiffusion coefficient.[14] While it is often assumed that phase separation between P3HT and PCBM to form the BHJ microstructure is due to the immiscibility of these components in liquid or amorphous states, the observation of interdiffusion demonstrates significant miscibility and complete mixing in our bilayer system at typical annealing temperatures (i.e. > 120 ° C). From these studies, we estimate that PCBM has a concentration greater than 40% wt in P3HT, which is consistent with previously reported estimates for bulk samples.[22] We believe that PCBM is dispersed as both molecular species within the disordered phase of P3HT (as shown below) and as aggregated PCBM domains. The observation of a fast interdiffusion coefficient indicates that the BHJ morphology formed after deposition will continue to change even under mild heating thus further complicating the characterization of its morphology.

## 2.3. Evolution of Molecular Ordering During Interdiffusion

The DSIMS profiles demonstrate the kinetics and temperature dependence of interdiffusion, but do not provide insight into the evolution of molecular ordering of P3HT and PCBM. Thus, 2-D X-ray scattering in grazing incidence geometry (GIWAXS) was used to understand the development of the crystal structure of P3HT and PCBM during the interdiffusion process. These measurements were taken with an X-ray incidence angle above the critical angle for total reflection of the P3HT and PCBM but below that of the Si substrate, thus probing the molecular ordering of the entire thickness of the bilayer sample. The scattering vectors in the out-of-plane and in-plane direction are denoted as q_z and q_{xy} respectively. 2D GIWAXS patterns were collected from as-prepared P3HT/PCBM bilayers and annealed samples allowing for direct comparison between the DSIMS profiles (**Figure 3a–e**). The packing along the side chains of the P3HT crystal is denoted as the a-axis, (h00), and the direction corresponding to the π-stacking within the P3HT crystal is denoted as the b-axis, (0k0). The diffraction peaks for P3HT were observed in the bilayer films with the (100), (200), and (300) found near the meridian (close to q_z) at q = 0.39, 0.77, 1.15 Å^{-1} respectively and the (010) near the horizon (along q_{xy}) at q = 1.65 Å^{-1}. This diffraction pattern shows that the a-axis of the P3HT crystals is predominantly oriented perpendicular to the substrate and the b-axis (π-stacking) is oriented parallel, which is the typically observed P3HT orientation. The diffuse ring centered at 1.41 Å^{-1} corresponds to the scattering of the disordered PCBM film initially found in the bottom layer of the bilayer.[23] Upon annealing the as-prepared bilayer system at various temperatures, the d-spacing along the a-axis of the P3HT

crystal remains constant, indicating that during the interdiffusion process, the PCBM does not interpenetrate between the side chains of the P3HT crystal structure.[24] Furthermore, the peak width of the diffraction ring corresponding to aggregates of PCBM is unchanged during the interdiffusion process, signifying that mixed PCBM remains in an amorphous state with aggregates large enough to scatter incident X-rays. Although the intensity of the (200) peak of P3HT increases by nearly a factor of two on annealing at 170 °C, its dependence on azimuthal angle at various levels of interdiffusion reveals that there is little change in the distribution of P3HT crystal orientations (Figures S8 and S9 in the Supporting Information). Because the d-spacing and orientations of P3HT crystals remained unchanged, it is clear that the interdiffusion process has little effect on the crystalline regions of the P3HT film. This data directly indicates the diffusion of PCBM in P3HT must occur within the disordered regions of P3HT.

To determine how interdiffusion within this system affects the growth of the P3HT crystallites, the P3HT crystallite size along the a-axis for the bilayer films was compared to pure P3HT films heated under similar conditions. The P3HT crystallite size was estimated using the Scherrer equation (from the peak width of diffraction corresponding to the (100) reflection of P3HT of annealed bilayer samples) and plotted against the fraction of PCBM within the P3HT layer (Figure 3f) (See Supporting Information). The crystallite size increases with increasing annealing temperature regardless of the level of interdiffusion, again supporting the idea that the diffusion of PCBM must occur within the disordered regions of P3HT. Furthermore, 2D GIWAXS patterns were collected from as-prepared bilayer samples heated in-situ at 110 °C and 170 °C for various times, thus allowing for the investigation of systems that range from partially mixed (~30 wt% PCBM in P3HT) to fully mixed during the time scale of this experiment. We also measured the crystal size along the (h00) direction for a neat P3HT film annealed in-situ after 5 min at 110 °C and 170 °C. The P3HT crystallite size in the bilayer system increased most rapidly during the first 5 min of annealing, growing to a thickness close to that for a neat P3HT film heated under similar conditions (Figure 3g). Thus, it is clear that the interdiffusion of PCBM and P3HT has little effect on both the size of the P3HT crystallites and the rate of crystal growth within the film.

2.4. Vertical Composition During Interdiffusion Using GIWAXS

Even though GIWAXS is a widely used technique to determine the crystal structure of thin films, its depth profiling capabilities has yet to be extensively explored in this context.[25] In order to explore the depth profile, the X-ray incidence angle onto the sample was less than the critical angle for the PCBM film (at ~0.10° incidence). In this case, only the top ~10 nm of the 265 nm thick P3HT film on top of PCBM was examined. For direct comparison, the sample stage was preheated to 170 °C prior to performing the experiment thus mimicking the exact annealing conditions of earlier discussed samples. The 2D GIWAXS patterns of the PCBM/P3HT bilayer, measured before heating, at 170 °C, and after cooling to room temperature are found in **Figure 4a–c**. The as-prepared bilayer measured below

Materials Views
www.MaterialsViews.com

ADVANCED
ENERGY
MATERIALS
www.advenergymat.de
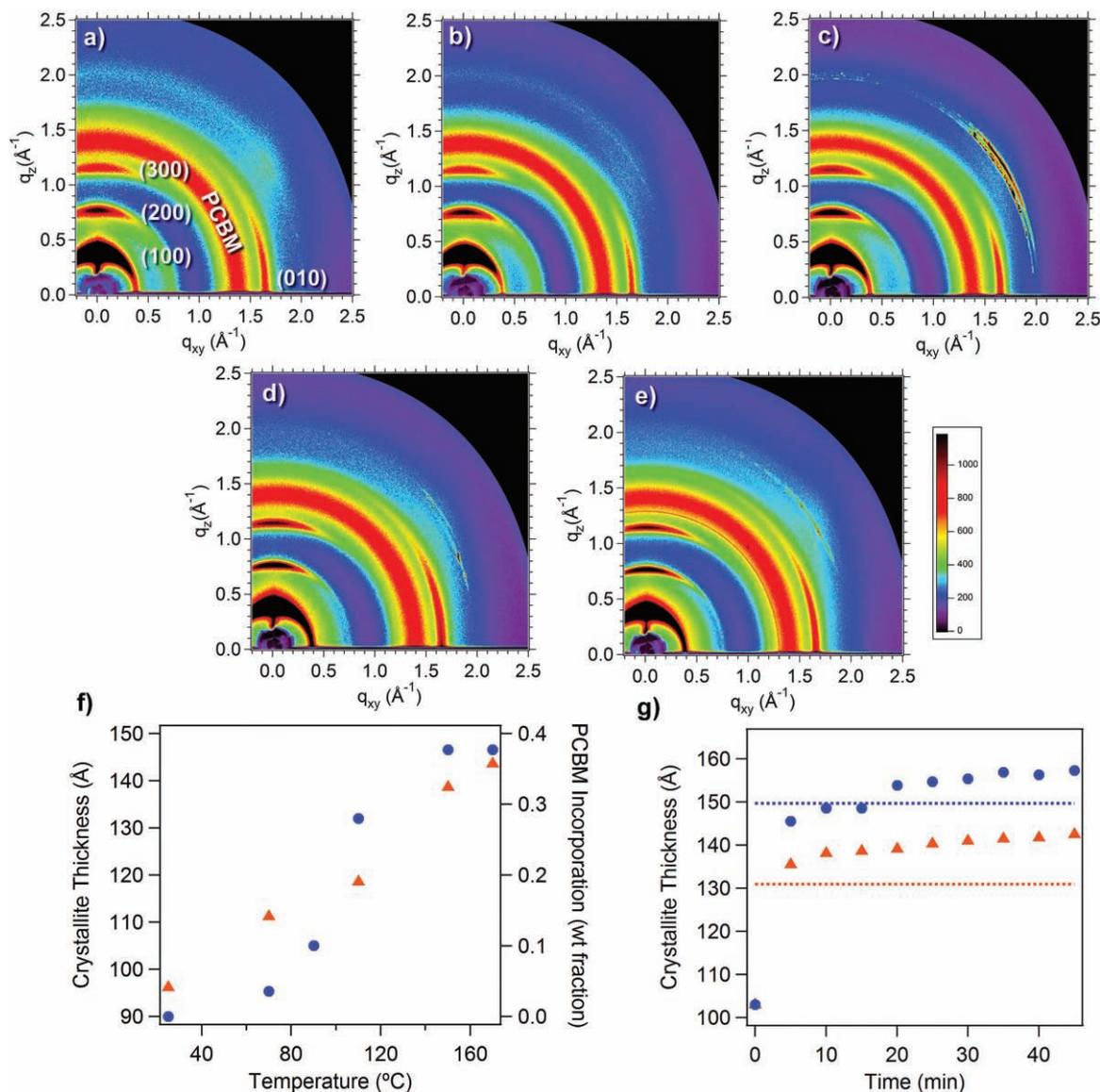
Figure 3. Two-dimensional GIWAXS of a P3HT/PCBM bilayer on Si a) as-cast and annealed at b) 70 °C, c) 110 °C, d) 150 °C, and e) 170 °C for 5 min. f) The Scherrer equation was used to extract the P3HT crystallite thickness along the a-axis from the full-width-at-half-maximum of the (100) reflection. PCBM incorporation from the DSIMS measurements was plotted for comparison at various annealing temperatures. g) Growth in the crystal thickness with time using in-situ heating 2D GIWAXS of a P3HT/PCBM bilayer on Si at 110 °C (orange) and 170 °C (blue). The Scherrer equation was used to determine crystal thickness from the (100) reflection corresponding to P3HT. The dotted line corresponds to a neat P3HT/Si sample heated for 5 min at 110 °C (orange) and 170 °C (blue).

the critical angle showed an identical diffraction pattern as a neat film of P3HT, signifying that only the top layer of the bilayer was probed (Figure S11 in the Supporting Information). Upon heating, the characteristic diffuse PCBM scattering ring centered at 1.41 Å^{-1} was observed, demonstrating that interdiffusion of P3HT and PCBM occurs in less than 5 min. The integrated out-of-plane scattering clearly shows the growth of the PCBM diffraction ring as well as the narrowing of the (h00) peaks corresponding to the increase in crystal thickness of P3HT along the a-axis (Figure 4d). The (h00) peak position shift to lower values of **q** observed in the bilayer scattering pattern at 170 °C is due to thermal expansion of the P3HT unit cell.[26] This experiment confirms that the interdiffusion

process is complete in less than 5 min at temperatures greater than 150 °C.[27] Furthermore, the d-spacing along the a-axis and orientation of P3HT crystals remains unchanged during the interdiffusion process and supports the conclusion that PCBM diffuses within the disordered regions of P3HT without significantly disrupting the P3HT crystallites.

2.5. Discussion

In contrast to previous reports, our results support the idea that the presence of PCBM within disordered P3HT has little influence on the increase in the number and size of P3HT crystallites
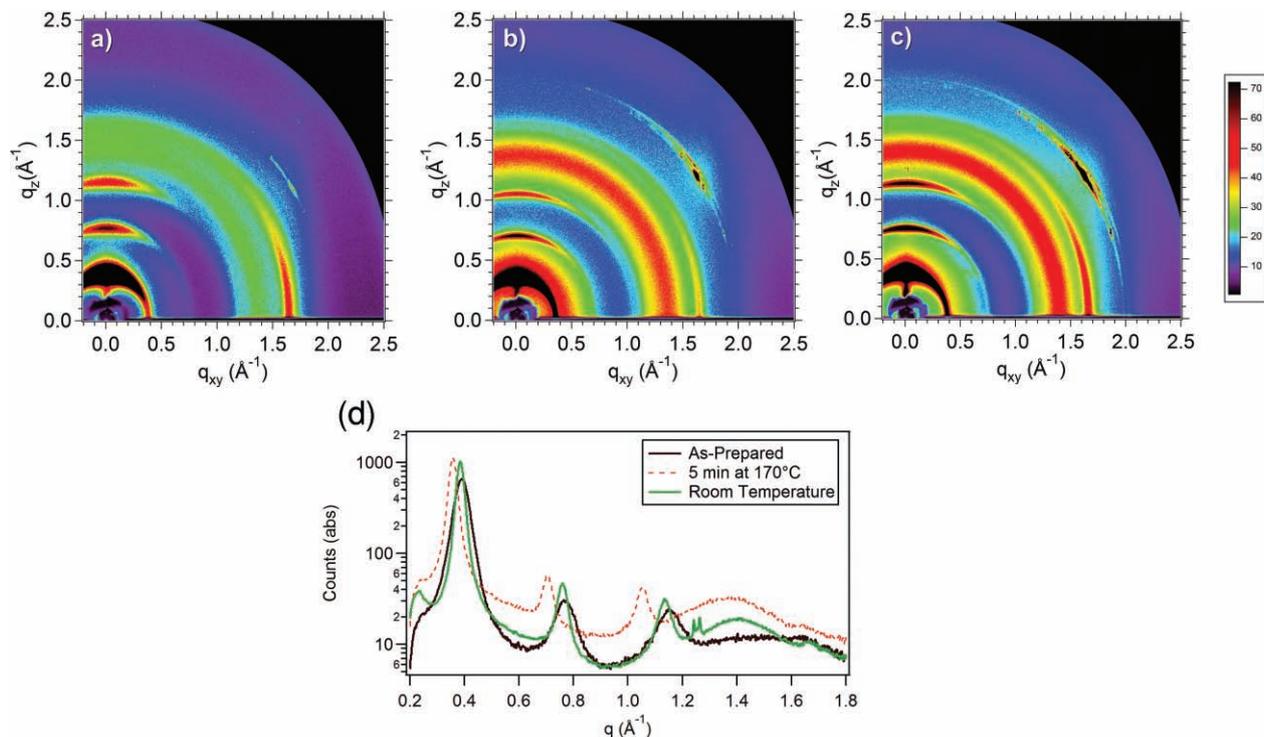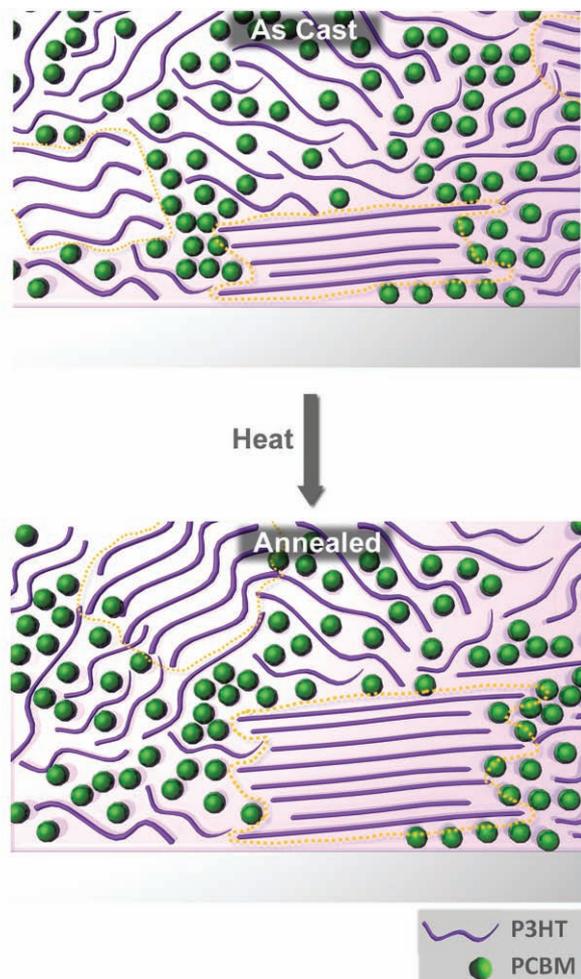
Figure 4. Two-dimensional GIWAXS of a P3HT/PCBM bilayer on Si oriented at ~0.10° incidence relative to the beam a) as-cast, b) measured in-situ at 170 °C for 5 min, and c) at room temperature after 35 min of annealing at 170 °C. d) Integrated out-of-plane scattering measured at room temperature (black), at 170 °C for 5 min (red), and at room temperature after 35 min of annealing at 170 °C (green).

during thermal annealing. Yang et al. speculate that the growth of P3HT fibrils during the thermal annealing process limits the growth of PCBM to nanometer-sized crystals. Others believe that the dispersion of PCBM within the P3HT inhibits the aggregation and crystallization of P3HT. Upon thermal annealing, they believe that the PCBM diffuses out of the P3HT to form larger aggregates and enables the disordered P3HT to crystallize.[5,28] In all cases, the authors of these previous studies speculate that the local concentration of P3HT and PCBM during annealing impacts the final BHJ morphology. However, it is clear from the results above that the growth of the P3HT crystallites upon annealing is likely independent of the interdiffusion process and thus the local concentration of PCBM. It is likely that the disagreements arose from the fact that all previous studies were performed using a P3HT:PCBM BHJ, which, due to the small length scale of phase separation, is challenging to characterize directly. We are not aware of any reports of the percentage of crystallinity for thin films of regioregular P3HT, but the results here suggest that the total crystallinity in the P3HT film is low based upon simple consideration of the volume change during the mixing process.[22] As depicted in **Figure 5**, the initial BHJ comprises a distribution of P3HT crystallites, PCBM aggregates, and a dispersion of PCBM (both molecular and small aggregates) in disordered P3HT. Upon annealing, our studies suggest that the size of the P3HT crystallites increases mainly within the first 5 min of annealing regardless of the local concentration of PCBM (at approximately a 1:0.8 wt ratio) while the PCBM aggregates remain dispersed in the disordered regions of P3HT. Thus, it can be speculated that the increase in the device

performance commonly observed during thermal annealing of P3HT:PCBM BHJs is mostly due to the increase in P3HT crystallite thickness, which should lead to improved hole transport within this system.

3. Conclusions

By using a bilayer of P3HT and PCBM, fast interdiffusion of these two components was observed at low temperatures, resulting in a homogeneous system when annealed at 150 °C for 30 s with an estimated interdiffusion coefficient of 3×10^{-10} cm^2/s. The fact that there is a clear drive towards a homogeneous mixture of P3HT and PCBM from a distinctly heterogeneous structure strongly suggests that PCBM (molecular or aggregated species) is dispersible (greater than 40 wt%) in disordered P3HT under typical annealing conditions of BHJ OPV. The observation of a fast interdiffusion rate indicates that the PCBM within the bulk heterojunction active layer has significant mobility in 3-dimensions, even under mild heat treatments, which further complicates the complete characterization of the morphology and interfacial compositions. Furthermore, it was found that the diffusion of PCBM within P3HT occurs within the disordered phases of P3HT having little effect on the growth of the P3HT crystallites. These results provide evidence that the fullerene phase of a BHJ is most likely either aggregated and/or molecularly dispersed within the disordered regions of P3HT.[29] While the studies here are specific to P3HT and PCBM, it is clearly of importance to determine the generality

© 2011 WILEY-VCH Verlag GmbH & Co. KGaA, Weinheim

Materials
Views

www.MaterialsViews.com

ADVANCED
ENERGY
MATERIALS

www.advenergymat.de

FULL PAPER

Figure 5. Schematic representation of the evolution of the P3HT:PCBM bulk heterojunction morphology upon thermal annealing. Crystalline domains of P3HT are surrounded by the yellow dotted lines. Our results support the idea that the P3HT crystal thickness increases with thermal annealing regardless presence of PCBM (at a 1:0.8 wt. ratio). It is also believed that the PCBM is distributed within the disordered P3HT regions even after thermal annealing.

of the results to other polymers with differing molecular structures. The methodology reported here is general, however, and can be applied to other polymers of interest, such as those with lower optical gaps.

4. Experimental Section

Sample Fabrication: Regioregular P3HT and PCBM were obtained from Merck Chemicals and Nano-C (Westwood, MA), respectively, and used as received. P3HT and PCBM solutions were both prepared using chlorobenzene (30 mg mL^{-1}) and stirred overnight at 70 °C to promote complete dissolution. All substrates were washed in an ultrasonic bath with acetone, 2% wt soap in water, deionized water, and 2-propanol for 20 min each and dried with nitrogen. P3HT and PCBM films were fabricated by spin-coating 30 mg/mL solutions in chlorobenzene at 800 rpm for 80 s in an inert environment at room temperature on a silicon substrate yielding thicknesses of 265 nm and 180 nm respectively. Films were allowed to age for two days in an inert environment before

bilayer fabrication. Bilayers were fabricated by floating a P3HT film onto a PCBM film. P3HT films were immersed in an HF:DI-water solution (1:19 by vol.) solution and floating onto a deionized-water surface. The free-standing P3HT film on water was then picked up by the neat supported PCBM film on either Si (GIWAXS and SEM) or SiO$_2$/Si (DSIMS) substrates. Films were then placed under vacuum (10^{-1} mbar) for 30 min to ensure proper film formation. A polystyrene layer was floated on all DSIMS samples after annealing for etch rate calibration. Deuterium abundance levels were calibrated with the use of DSIMS depth profile measurements on a PS/d-PS/PS trilayer on SiO$_2$/Si. All PS films were spun-cast from toluene (25 mg mL^{-1}).

Characterization: A Physical Electronics 6650 Quadropole dynamic SIMS was used to obtain depth profiles of the films on SiO$_2$/Si substrates. The substrates were cooled on a cryostage for 30 min prior to analysis. A 2kV O$_2^+$ beam at ~45 nA was rastered across a 200 μm × 200 μm area, of which only the middle 15% was analyzed for composition by collecting negative secondary ions.

Scanning electron microscopy (SEM) images were acquired using an FEI XL30 Sirion FEG digital electron scanning microscope. All cross-section samples were prepared by immersion in liquid nitrogen followed by fracture.

2D GIWAXS were performed at the Stanford Synchrotron Radiation Laboratory on beamline 11–3 with an area detector, MAR345 image plate, at grazing and specular incidence with an incident energy of 12.7 keV. The samples were kept under a helium atmosphere during irradiation to minimize X-ray beam damage. Films were typically exposed for 80 s at an incidence angle of about 0.10° – 0.12°.

Supporting Information

Supporting Information is available from the Wiley Online Library or from the author.

Acknowledgements

[1] H. Y. Chen, J. H. Hou, S. Q. Zhang, Y. Y. Liang, G. W. Yang, Y. Yang, L. P. Yu, Y. Wu, G. Li, *Nat. Photonics* **2009**, 3; b) J. Peet, A. J. Heeger, G. C. Bazan, *Acc. of Chem. Res.* **2009**, *42*, 1700–1708.

[2] This result is consistent with a recent hypothesis in E. D. Gomez, K. P. Barteau, H. Wang, M. F. Toney, Y.-L. Loo, *Chem. Comm.* **2010** DOI: 10.1039/C0CC02927K.

[3] M. C. Scharber, D. Wuhlbacher, M. Koppe, P. Denk, C. Waldauf, A. J. Heeger, C. L. Brabec, *Adv. Mater.* **2006**, *18*, 789–795.

[4] B. C. Thompson, J. M. J. Frechet, *Angew. Chem., Int. Ed* . **2008**, *47*, 58–77.

[5] a) W. L. Ma, C. Y. Yang, X. Gong, K. Lee, A. J. Heeger, *Adv. Funct. Mater.* **2005**, *15*, 1617–1622; b) G. Li, V. Shrotriya, Y. Yao, Y. Yang,

www.MaterialsViews.com

ADVANCED
ENERGY
MATERIALS
www.advenergymat.de

FULL PAPER

J. App. Phys., **2005**, *98*, c); Y. Kim, Y. Kim, S. A. Choulis, J. Nelson, D. D. C. Bradley, S. Cook, J. R. Durrant, *App. Phys. Lett.* **2005**, *86*.

[6] F. Padinger, R. S. Rittberger, N. S. Sariciftci, *Adv. Funct. Mater.* **2003**, *13*, 85–88.

[7] M. Campoy-Quiles, T. Ferenczi, T. Agostinelli, P. G. Etchegoin, Y. Kim, T. D. Anthopoulos, P. N. Stavrinou, D. D. C. Bradley, J. Nelson, *Nat. Mater.* **2008**, *7*, 158–164.

[8] a) X. N. Yang, J. K. J. van Duren, M. T. Rispens, J. C. Hummelen, R. A. J. Janssen, M. A. J. Michels, J. Loos, *Adv. Mater.* **2004**, *16*, 802-806; b) M. T. Rispens, A. Meetsma, R. Rittberger, C. J. Brabec, N. S. Sariciftci, J. C. Hummelen, *Chem. Commun.* **2003**, 2116–2118.

[9] D. Chirvase, J. Parisi, J. C. Hummelen, V. Dyakonov, *Nanotechnology* **2004**, *15*, 1317–1323.

[10] S. Gunes, H. Neugebauer, N. S. Sariciftci, *Chem. Rev.* **2007**, *107*, 1324–1338.

[11] M. Reyes-Reyes, K. Kim, D. L. Carroll, *App. Phys. Let.* **2005**, *87*.

[12] J. Jo, S. I. Na, S. S. Kim, T. W. Lee, Y. Chung, S. J. Kang, D. Vak, D. Y. Kim, *Adv. Funct. Mater.* **2009**, *19*, 2398–2406.

[13] X. N. Yang, J. Loos, S. C. Veenstra, W. J. H. Verhees, M. M. Wienk, J. M. Kroon, M. A. J. Michels, R. A. J. Janssen, *Nano Lett.* **2005**, *5*, 579–583.

[14] B. Watts, W. J. Belcher, L. Thomsen, H. Ade, P. C. Dastoor, *Macromolecules* **2009**, *42*, 8392–8397.

[15] J. W. Kiel, B. J. Kirby, C. F. Majkrzak, B. B. Maranville, M. E. Mackay, *Soft Matter* **2010**, *6*, 641–646.

[16] W. Geens, T. Martens, J. Poortmans, T. Aernouts, J. Manca, L. Lutsen, P. Heremans, S. Borghs, R. Mertens, D. Vanderzande, *Thin Solid Films* **2004**, *451*, 498–502.

[17] A. L. Ayzner, C. J. Tassone, S. H. Tolbert, B. J. Schwartz, *J. of Phys Chem. C* **2009**, *113*, 20050–20060.

[18] a)T. A. M. Ferenczi, J. Nelson, C. Belton, A. M. Ballantyne, M. Campoy-Quiles, F. M. Braun, D. D. C. Bradley, *J. of Phys.:Condens. Matter* **2008**, *20*; b) D. E. Markov, E. Amsterdam, P. W. M. Blom,

A. B. Sieval, J. C. Hummelen, *J. of Phys. Chem. A* **2005**, *109*, 5266–5274.

[19] a) C. M. B. Svanstrom, J. Rysz, A. Bernasik, A. Budkowski, F. Zhang, O. Inganas, M. R. Andersson, K. O. Magnusson, J. J. Benson-Smith, J. Nelson, E. Moons, *Adv. Mater.* **2009**, *21*, 4398–4403; b) C. W. T. Bulle-Lieuwma, W. J. H. van Gennip, J. K. J. van Duren, P. Jonkheijm, R. A. J. Janssen, J. W. Niemantsverdriet, *Appl. Surf. Sci.* **2003**, *203*, 547–550.

[20] a)W. J. Zeng, K. S. L. Chong, H. Y. Low, E. L. Williams, T. L. Tam, A. Sellinger, *Adv. Funct. Mater.* **2009**, *19*, 1227–1234; b) D. S. Germack, C. K. Chan, B. H. Hamadani, L. J. Richter, D. A. Fischer, D. J. Gundlach, D. M. DeLongchamp, *App. Phys. Let.* **2009**, *94*, 233303.

[21] R. A. Segalman, A. Jacobson, E. J. Kramer, S. R. Lustig, *Macromolecules* **2004**, *37*, 2613–2617.

[22] J. Y. Kim, D. Frisbie, *J. of Phys. Chem. C* **2008**, *112*, 17726–17736.

[23] The powder like diffraction occurring at ~2.0 Å^{-1} corresponds to the (111) reflection of Si residue from the sample preparation.

[24] A. C. Mayer, M. F. Toney, S. R. Scully, J. Rivnay, C. J. Brabec, M. Scharber, M. Koppe, M. Heeney, I. McCulloch, M. D. McGehee *Adv. Funct. Mater.* **2009**, *19*, 1173–1179.

[25] R. F. Saraf, C. Dimitrakopoulos, M. F. Toney, S. P. Kowalczyk, *Langmuir* **1996**, *12*, 2802–2806.

[26] E. Verploengen, R. Mondal, C. J. Bettinger, S. Sok, M. F. Toney, Z. Bao, *Adv. Funct. Mater.* In Press.

[27] Shorter time periods could not be investigated with GIWAXS due to the time required to align the sample.

[28] a) T. Erb, U. Zhokhavets, G. Gobsch, S. Raleva, B. Stuhn, P. Schilinsky, C. Waldauf, C. J. Brabec, *Adv. Funct. Mater.* **2005**, *15*, 1193–1196; b) G. Dennler, M. C. Scharber, C. J. Brabec, *Adv.Mater.* **2009**, *21*, 1323–1338.

[29] J. S. Moon, J. K. Lee, S. N. Cho, J. Y. Byun, A. J. Heeger, *Nano Letters* **2009**, *9*, 230–234.